Piezoelectrically-activated antibacterial catheter for prevention of urinary tract infections in an on-demand manner

Xiaofeng Duan [a,1], Yongde Xu [b,1], Zhifa Zhang [c,1], Xinbo Ma [d], Cui Wang [e], Wenjing Ma [e], Fan Jia [a], Xiaoying Pan [f], Yang Liu [f], Yantao Zhao [d,*], Qihong Li [g,**], Zhiqiang Liu [e,***], Yong Yang [f,****]

[a] Department of Urology, The Third Affiliated Hospital of Jinzhou Medical University, Jinzhou, Liaoning, 121000, China
[b] Department of Urology, Beijing Friendship Hospital, Capital Medical University, Beijing, 100050, China
[c] Department of Neurosurgery, The First Medical Center of Chinese PLA General Hospital, Beijing, 100853, China
[d] Senior Department of Orthopedics, The Fourth Medical Center of PLA General Hospital, No. 51, Fucheng Road, Haidian District, Beijing, 100048, China
[e] Beijing Institute of Basic Medical Sciences, No. 27 Taiping Road, Haidian District, Beijing, 100850, China
[f] Department of Urology, The Affiliated Hospital of Changchun University of Chinese Medicine, Changchun, Jilin, 130021, China
[g] Department of Stomatology, The Fifth Medical Center, Chinese PLA General Hospital, Beijing, 100071, China

ABSTRACT

Catheter-associated urinary tract infection (CAUTI) is a common clinical problem, especially during long-term catheterization, causing additional pain to patients. The development of novel antimicrobial coatings is needed to prolong the service life of catheters and reduce the incidence of CAUTIs. Herein, we designed an antimicrobial catheter coated with a piezoelectric zinc oxide nanoparticles (ZnO NPs)-incorporated poly-vinylidene difluoride-hexafluoropropylene (ZnO-PVDF-HFP) membrane. ZnO-PVDF-HFP could be stably coated onto silicone catheters simply by a one-step solution film-forming method, very convenient for industrial production. *In vitro*, it was demonstrated that ZnO-PVDF-HFP coating could significantly inhibit bacterial growth and the formation of bacterial biofilm under ultrasound-mediated mechanical stimulation even after 4 weeks. Importantly, the on and off of antimicrobial activity as well as the strenth of antibacterial property could be controlled in an adaptive manner via ultrasound. In a rabbit model, the ZnO-PVDF-HFP-coated catheter significantly reduced the incidence CAUTIs compared with clinically-commonly used catheters under assistance of ultrasonication, and no side effect was detected. Collectively, the study provided a novel antibacterial catheter to prevent the occurrence of CAUTIs, whose antibacterial activity could be controlled in on-demand manner, adaptive to infection situation and promising in clinical application.

1. Introduction

Urethral catheters are one of the most commonly used medical consumables in the clinic and have a wide range of applications [1]. However, catheter-associated urinary tract infections (CAUTIs) are the most common complication during catheterization, accounting for 23 % of intensive care unit (ICU) infections and 40 % of hospital-wide infections [2–4]. It was found that the incidence of CAUTIs is 100 % when indwelling catheters are implanted for more than 1 month [5]. Thirty percent of patients with indwelling catheters developed genitourinary or systemic symptoms as a result of CAUTIs, and about 4 % developed bacteremia, with a mortality rate of up to 30 % in this case [6]. Infections caused by indwelling urinary catheters are consisderred as a serious public health event, ranking fourth among the causes of nosocomial infection [7]. The indwelling catheter provides a convenient channel for pathogenic microorganisms to enter the urinary tract [8].

Scheme 1. Schematic illustrating the preparation process and application of ZnO-PVDF-HFP antimicrobial coated catheters.

Bacteria that enter the urinary tract can adhere, colonize, and eventually form biofilms on the surface of the catheter [9,10]. The biofilm on the surface of the catheter constitutes a barrier that protects the bacteria, which can diminish the therapeutic effect of antibiotics [11]. Therefore, CAUTIs are prone to recurrence and even drug resistance after treatment.

Ideally, catheters that are left in the body should have stable and adaptive antimicrobial effect, whose antibacterial activity could be adjusted according to the occurrence and levels of CAUTIs [12,13]. Currently, it mainly depends on their inherent antibacterial properties for some antimicrobial catheters to prevent CAUTIs. Silver ion hydrophilic coating and antibiotic-eluting catheters are common antibacterial method for clinical catheters. However, silver ion hydrophilic coating catheters cannot be adjusted according to infection conditions [14], and clinically, their antimicrobial effectiveness does not appear significant [15]. Antibiotic-eluting catheters have shown some improvement, but there are problems of antibiotic resistance and rapid depletion [16–18]. Some promising antimicrobial methods have not yet been widely used in the clinic, such as antimicrobial peptide (AMP) coated catheters. AMPs are broad-spectrum antimicrobial agents against Gram-negative, Gram-positive bacterial strains, viruses, and fungi. However, AMPs coatings still face challenges such as loss of antimicrobial activity, nonspecific binding, and alterations in peptide orientation [19]. Additionally, researchers are exploring the use of hydrogels as carriers to load furanone derivatives antimicrobial agents onto urinary catheters, demonstrating better antimicrobial effects compared with traditional Foley catheters [20]. Actually, most of antimicrobial catheters currently under research rely on antimicrobial drugs [21]. Piezoelectric materials can convert mechanical stimulation into electrical current with potential antibacterial effects [22] through controlled stimulus signals, such as ultrasound. For example, it was reported that the growth of *Escherichia coli* (E.coli) was significantly inhibited when ultrasound was applied to piezoelectric films made of PVDF-HFP and PVDF-TrFE [23,24]. More importantly, the on and off of the antibacterial activity could be controlled via ultrasound as well as the strength of antibacterial ability for piezoelectric materials, adaptive to the needs of infection levels and without developing drug resistance [25]. However, there is yet no such an antimicrobial catheter at present.

Based on these considerations, this study developed a piezoelectrically-activated antibacterial catheter using ZnO NPs-incorporated PVDF-HFP to form an antimicrobial coating on the surface of a silicone catheter simply through one-step film-forming method. During catheterization, ultrasonic stimulation could be employed in an on-demand manner to inhibit the potential infection and biofilm formation, preventing the occurrence of CAUTIs and clearing existing infections (Scheme 1).

2. Experimental section

2.1. Materials

Polyvinylidene fluoride-hexafluoropropylene (PVDF-HFP, Mn = 1.3 $\times 10^5$ g/mol) was purchased from Sigma-Aldrich (U.S.A.). N–N dimethylformamide (DMF, analytical grade) was purchased from Beijing psaitong Biotechnology Co. Acetone (Acetone, analytical grade), Zinc oxide nanoparticles (ZnO NPs, analytical grade), and phosphate buffered saline (PBS, analytical grade) were purchased from Aladdin China Co. *Escherichia coli* (*E. coli*, CMCC 44829) and *Staphylococcus aureus* (*S. aureus* CMCC 26001) were purchased from the Center for the Management of Chinese Medicine Strain Collection. Mouse skin fibroblasts (L929) (iCell-m026) were purchased from iCell Biosciences (Shanghai, China). 0.5 % trypsin-EDTA and penicillin-streptomycin were purchased from (Gibico, U.S.A). CCK-8 assay kit was purchased from Novozymes Bioscience (Nanjing, China), Bacterial viability assay kit (40274ES60) and reactive oxygen species assay kit (50101ES01) were purchased from Novozymes Bioscience (Nanjing, China). ROS (Reactive Oxygen Species) kit (50101ES01) was purchased from yeasan Biotech (Shanghai, China). Interleukin- 6 (IL-6) was purchased from Google Biotech Inc (Wuhan, China). Tumor necrosis factor-α (TNF-α) was purchased from BOSTER Biological Technology Co (Wuhan China). Hematoxylin-eosin stain (H&E) was purchased from Wuhan Baiqiandu Biotechnology Co. Fr12 size silicone Foley catheter (UC) was purchased from Jiangxi Yikang Medical Equipment Group Co.

2.2. Preparation of ZnO-PVDF-HFP antimicrobial coated urinary catheters

A 20 % PVDF-HFP solution was prepared. The solvent was a solution of acetone mixed with DMF at the ratio of 2:3. 1 mg/ml Zinc oxide nanoparticles were added to the stirred PVDF-HFP solution. The Fr12 silicone catheter was immersed in the coating solution overnight at 4 °C. Then, the catheter was retrieved and placed in a vacuum drying oven at 60 °C for 5 h. After drying, a uniform film was formed on the surface of catheter. Finaly, the dried catheter was annealed for 12 h at a temperature of 120 °C.
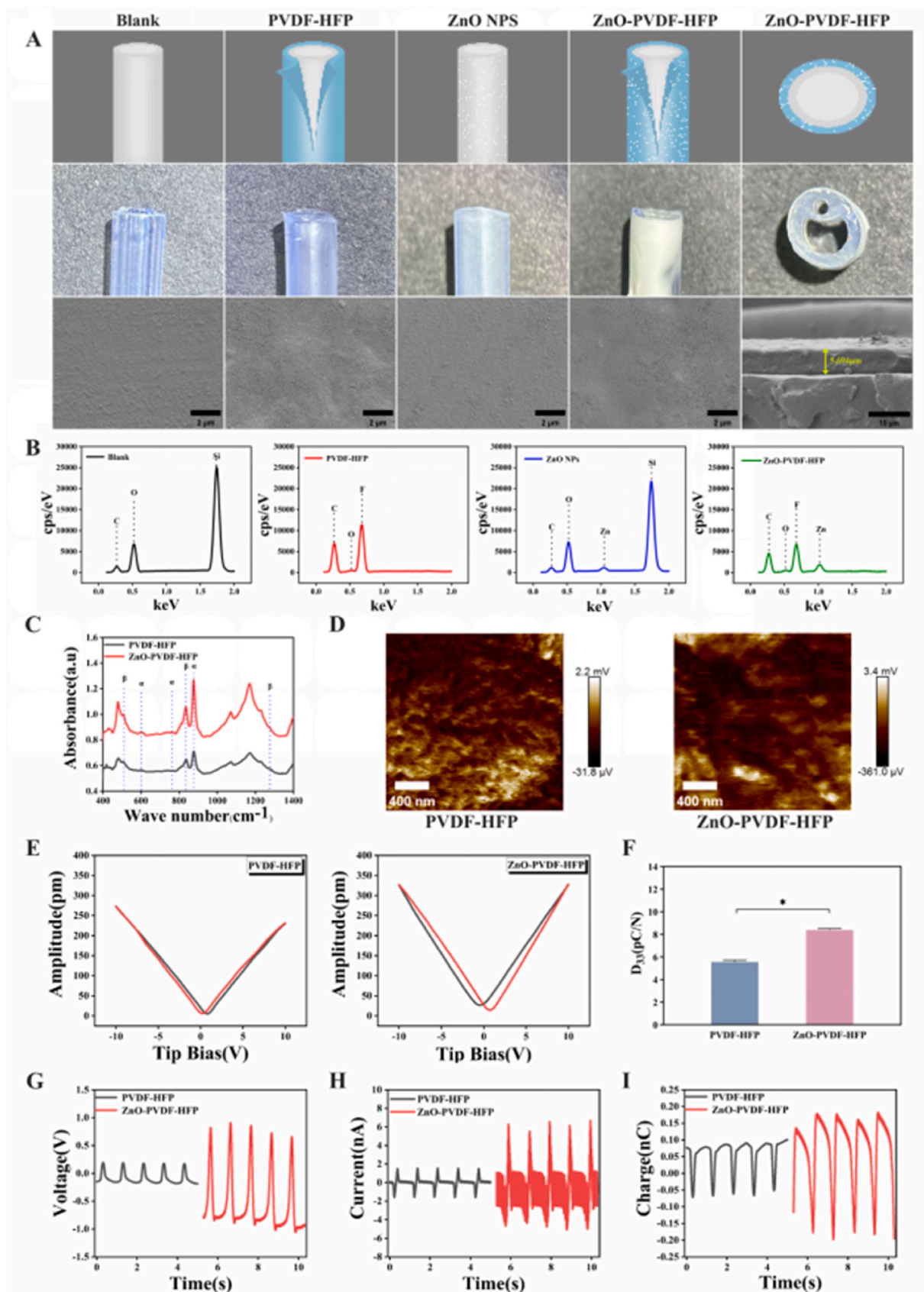
Fig. 1. Physical properties of piezoelectric antimicrobial ZnO-PVDF-HFP coated catheters. (A) Pattern maps, physical photographs and SEM images of catheter samples of Blank group, PVDF-HFP group, ZnO NPs group, and ZnO-PVDF-HFP group, (B) EDS results, (C) FTIR results, (D) PFM images, (E) Butterfly curves, (F) D_{33} piezoelectricity coefficient results (G) Output voltages, (H) Short circuit currents, (I) Output charge. All statistics are expressed as mean ± standard deviation (* indicate statistical differences between PVDF-HFP-coated catheters and ZnO-PVDF-HFP-coated ones; *$P < 0.001$).

2.3. Physicochemical characterization of ZnO-PVDF-HFP coated catheters

The surface morphology and elemental composition of the ZnO-PVDF-HFP coated catheters were tested by using scanning electron microscope (SEM, Gemini, ZEISS, Germany) combined with energy dispersive Energy dispersive spectroscopy (EDS). The prepared ZnO-PVDF-HFP catheters were cut into 2.5-cm-long segments and then analyzed by Fourier Transform Infrared Spectroscopy (FTIR, Thermo, Scientific Nicolet, US). Piezoelectric outputs of the ZnO-PVDF-HFP coating catheters were measured under an impact force of 20.0 N through a high impedance electrometer (Keithley 6517B, Cleveland, USA). The ZnO-PVDF-HFP coating catheters were characterized and morphologically imaged at high resolution and piezoelectric response curves were obtained using an atomic force microscope (AFM, Bruker, Dimension Icon, Germany) in PFM mode. The piezoelectric constant (D_{33}) of the coating was measured using a D_{33} tester (ZJ-3A, CHINA).

2.4. In vitro antimicrobial properties of ZnO-PVDF-HFP coated catheters

The antimicrobial activity of the coated catheter was tested by bacterial fluid of E.coli and S.aureus (1×10^6 CFU/ml). Then, the bacterial fluid was incubated at 37 °C. The experimental group was treated by ultrasonic wave (100 W for 1 h). Then, the absorbance value of the bacterial solution was measured at 600 nm using an enzyme marker. The bacterial concentration was determined by drop colony counting method. The bacterial morphology was observed with a biological scanning electron microscope. To evaluate the live and dead cells, the bacteria were stained using a live/dead bacterial staining kit (DMAO/ethD-III) and observed by fluorescence microscopy.

2.5. Stability of ZnO-PVDF-HFP coatings

The ZnO-PVDF-HFP coated catheters were immersed in human urine for 0, 7, 14, and 28 days. The adhesion of the coated catheter was detected by measuring the surface morphology as well as the elemental composition of the ZnO-PVDF-HFP coated catheter after immersion in urine. The stability of the ZnO-PVDF-HFP coated catheter was judged by detection of a high impedance electrometer and the optical density value of bacterial bacterial fluids.

2.6. ROS detection and anti-biofilm properties

The ZnO-PVDF-HFP coated catheters were co-cultured with E.coli and S.aureus and using ultrasound to stimulate ZnO-PVDF-HFP coated catheters for 1 h. The catheters were stained with ROS indicator DCFH-DA (10×10^{-6} M) for 15 min in the dark, and then the ROS production pattern was observed by fluorescence microscopy.

The catheters were co-cultured with the two bacteria for 7 days. Then using ultrasound to stimulate ZnO-PVDF-HFP coated catheters for 1 h per day. The catheters were fixed with paraformaldehyde for 0.5 h and dehydrated with an ethanol gradient. Finally, the bacterial biofilm formation was observed by bioscanning electron microscopy.

2.7. Biocompatibility

Fibroblasts L929 were used to evaluate the cytotoxicity of ZnO-PVDF-HFP coated catheters. The ZnO-PVDF-HFP coated catheter was immersed in cell culture medium for 24 h to obtain the supernate. The supernate was used to culture L929 cells, the cell viability was evaluated by CCK-8 assay kit and the cell morphology was observed using live/dead cell assay kit at 1 and 4 days after culture, respectively.

2.8. Animal experimentation

The in vivo antimicrobial effect of ZnO-PVDF-HFP coated catheters was evaluated. All the animal experiments were conducted in accordance with the Guide for the Care and Use of Laboratory Animals (National Institutes of Health Publication no. 80-23, revised 1996) and approved by the Beijing Long 'an Laboratory Animal Breeding Center and the Animal Ethics Committee of the Academy of Military Medical Sciences (Beijing, China). All experiments were conducted in the research facility of Beijing Long 'an Laboratory Animal Breeding Center. New Zealand white rabbits of 3–4 months old with an average body weight of 3 Kg were used as experimental animals (n = 12).

All animals were clinically examined and in good health at the beginning of the experiment. Catheterization was performed under general anesthesia after intramuscular injection of xylazine hydrochloride 4–6 mg/kg. After application of lubricant, catheters that had undergone UV irradiation were inserted aseptically into the urethra up to the bladder and the catheters were secured with sutures in the abdominal wall to prevent the animals from pulling the catheters out of the body. The urethra and bladder areas were ultrasonically stimulated for 10 min per day with a portable handheld ultrasound instrument with a power of 1w.

The vital signs of the animals were monitored during the experiment. All animals recovered well and no deaths were observed during anesthesia. At the end of the 7-day catheterization period, blood and urine were collect from the animals for further analysis. After collection of urine and blood, the experimental animals were euthanized, and the urethral and bladder tissues of the animals were removed, fixed with paraformaldehyde, and subjected to H&E staining and immunohistochemical staining.

2.9. Analyze statistics

All data are expressed as mean ± standard deviation (SD). For multiple comparisons, statistical analyses were performed using one-way analysis of variance (ANOVA) using GraphPad Prism software (version 8.0, San Diego, USA). Post hoc Tukey test or unpaired two-tailed t-test was then performed. p-values less than 0.05 were considered statistically significant.

3. Results and discussion

3.1. Characterization of ZnO-PVDF-HFP coated catheters

After vacuum drying, the catheters immersed in different solvents showed different morphologies (Fig. 1A and B). It could be seen that a transparent film structure was formed on the surface of the catheters treated by PVDF-HFP and the ZnO-PVDF-HFP, whereas white particulate matter was seen on ZnO NPs-treated ones only. The surface morphology of the catheters was observed using a high-resolution SEM, which showed that the a thin film of about 5 μm thick was formed on the surface of ZnO-PVDF-HFP-coated catheters. The elemental energy spectroscopy analysis confirmed the presence of fluorine and zinc, indicating that the ZnO NPs were successfully incorporated in the PVDF-HFP film. The surface of the ordinary silicone catheter was smooth and flat, and no membrane structure was observed; On the ZnO NPs-coated catheter, dots could be observed but membrane structure. EDS analysis showed the presence of zinc; the external surface of the PVDF-HFP-coated catheter was similar to that of the ZnO-PVDF-HFP-coated one, but no zinc was detected through the elemental analysis. It was shown that the adding 1 % ZnO NPs to 20 % PVDF-HFP solution would resulted in complexes with good piezoelectric properties [26,27]. Therefore, we used this method to prepare ZnO-PVDF-HFP coated catheters. It was also confirmed that this ratio of the mixed solution could allow ZnO-PVDF-HFP thin film to attach on silicone catheters stably.

To determine the β-phase ratio of ZnO-PVDF-HFP, the FTIR spectra of pure PVDF-HFP and ZnO-PVDF-HFP films in the spectral range of 400–1500 cm^{-1} were detected as shown in Fig. 1C. Absorption peaks at 603, 765, and 875 cm^{-1} are α-phase specific ones, while absorption
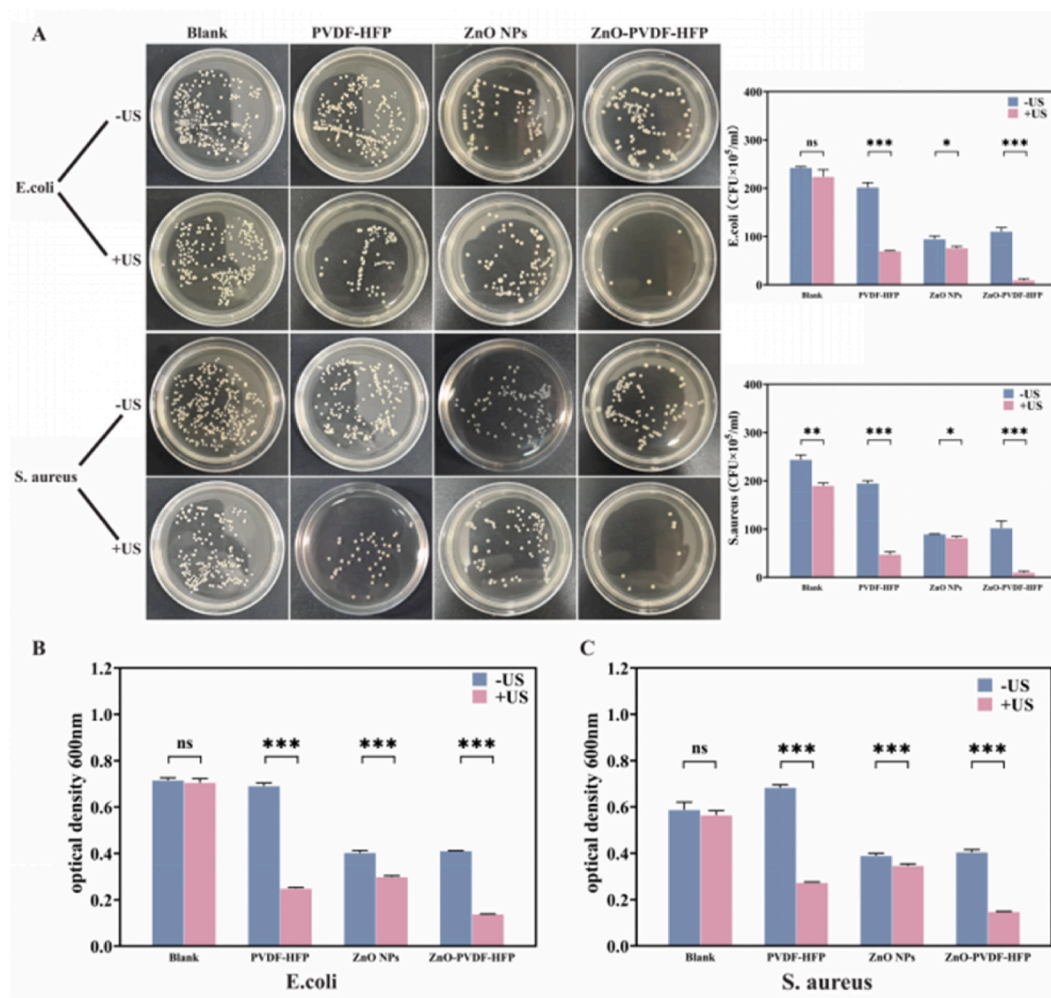
Fig. 2. *In vitro* **antimicrobial effect of different groups of catheters against Escherichia coli and Staphylococcus aureus.** (A) Colony counts in different groups, (B) Optical density values of *E.coli*, (C) Optical density values of *S. aureus* All statistics are expressed as mean ± standard deviation (* indicate statistical differences between different groups of catheters; *$P < 0.05$, **$P < 0.01$, ***$P < 0.0001$).

peaks at 510, 840, and 1270 cm^{-1} are β-phase specific ones. According to the previous report [28,29], the relative fraction F(β) of the β-phase can be calculated from **Equations 1** assuming that the IR follows the Beer-Lambert law：

$$F(\beta) = \frac{A(\beta)}{1.26A(\alpha) + A(\beta)}$$

where A(α) is the absorbance at 765 cm^{-1} and A(β) is the absorbance at 840 cm^{-1}. The calculation show that the β-phase fraction of pure PVDF-HFP is about 66.3 %, while the β-phase fraction of ZnO- PVDF-HFP increased to 76.8 %, which will lead to better piezoelectric properties. Many researchers have reported that the surface charges on the ZnO nanofillers interact with the molecular dipoles (CH$_2$ or CF$_2$) of PVDF-HFP and improves the β-phase content of the composites [30,31].

The piezoelectric properties of pure PVDF-HFP and ZnO-PVDF-HFP coatings were examined using AFM. Both PVDF-HFP and ZnO-PVDF-HFP showed significant piezoelectric activity, with the surface potentials of the films being about 2.2 mV and 3.3 mV(Fig. 1D). In addition, the well-known butterfly curve was shown in the AFM amplitude and phase plots, which is a characteristics of piezoelectric material(Fig. 1E) [32]. We evaluated the piezoelectric properties of pure PVDF-HFP films and ZnO-PVDF-HFP ones by measuring the D$_{33}$. As is shown in Fig. 1F, the piezoelectric coefficient of ZnO-PVDF-HFP film is 1.5 times higher than that of the PVDF-HFP one. The results indicated that adding ZnO NPs to PVDF-HFP can enhance its piezoelectric properties.

Output charges, currents and voltages of PVDF-HFP and ZnO-PVDF-HFP coatings were measured using a high impedance electrometer (Fig. 1G–I). The voltages of PVDF-HFP and ZnO-PVDF-HFP coatings were 0.16V and 0.9 V, the short-circuit currents were 1.55 nA and 3.98 nA, and the charges were 0.07 nC and 0.19 nC, respectively. The results showed that adding ZnO NPs into PVDF-HFP increased the output voltageas well as the currents and charges. This is because that doped ZnO nanoparticles may enhance the piezoelectric properties of the PVDF-HFP. In conclusion, we successfully prepared ZnO-PVDF-HFP antimicrobial coated catheters.

We used the solution film-forming method to prepare ZnO-PVDF-HFP thin film coatings, which has the advantages of low requirements for experimental equipment, simple process, and ease to operate with low cost. This method was reported previously by Chary [33], who used multi-walled carbon nanotubes (CNT) as a filler to cast a flexible composite membrane in a poly(vinylidene fluoride)-hexafluoropropylene polymer matrix. In the study, we confirmed that the method could also effectively form ZnO-PVDF-HFP films on the catheter surface without destroying the original catheter structure. In addition, adding ZnO nanoparticles to PVDF-HFP can enhance its piezoelectric properties. β-phase is a very favorable crystalline phase structure of PVDF-HFP with a higher degree of polarization, and thus is important for piezoelectric effects [34]. FTIR demonstrated that the addition of ZnO NPs increased the content of polar β-phase in PVDF-HFP, which should one of key causes for the improved piezoelectric properties of
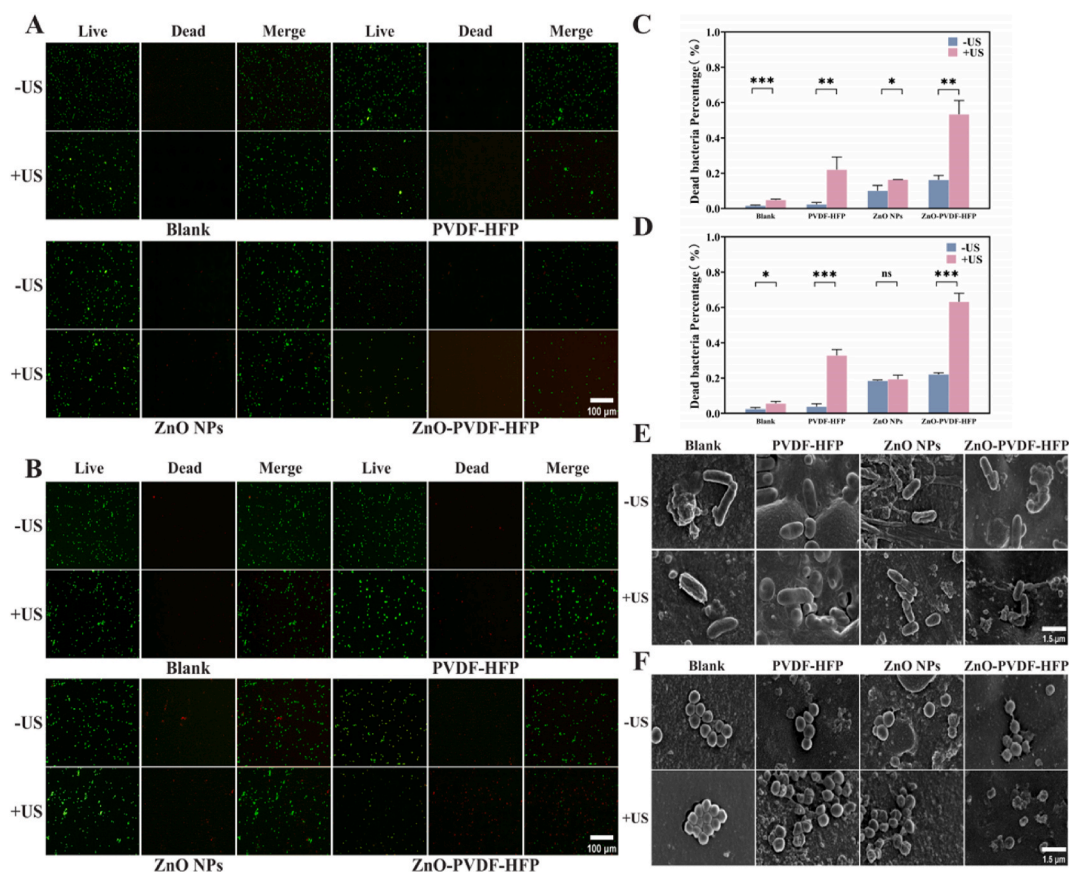
Fig. 3. *In vitro* antimicrobial effect of different groups of catheters. (A) Live/dead staining of *E. coli*, (B) Live/dead staining of *S. aureus*. (C) Bacterial death rate in different groups of *E. coli*. (D) Bacterial death rate in different groups of *S. aureus*. (E) SEM images of *E. coli*, (F) SEM images of *S. aureus*. All statistics are expressed as mean ± standard deviation (* indicate statistical differences between different groups of catheters; *$P < 0.05$, **$P < 0.01$, ***$P < 0.001$).

ZnO-PVDF-HFP thin films compared with PVDF-HFP.

3.2. In vitro antimicrobial activity of ZnO-PVDF-HFP coated catheters

E.coli and S.aureus are two common pathogens of urinary tract infections [35]. Thus, we chose these two bacteria for *in vitro* evaluation of antimicrobial capacity. The *in vitro* antibacterial experiments were divided into 8 groups, including Blank group, PVDF-HFP group, ZnO NPs group, ZnO-PVDF-HFP group, Blank + US group, PVDF-HFP + US group, ZnO NPs + US group and ZnO-PVDF-HFP + US group. Bacterial colony counting was performed for each group after treatment, the results were shown in Fig. 2A. The coated catheters exhibited a similar antimicrobial tendency against *E. coli* and *S. aureus*. The ZnO-PVDF-HFP + US group was counted with significantly fewer colony-forming unit （CFU） of *E. coli* and *S. aureus* compared with those in other groups. The CFU of the two bacteria in the ZnO-PVDF-HFP + US group were 9×10^5 CFU/ml and 10×10^5 CFU/ml, respectively. The colony counts of the bacteria in Blank group were 2.43×10^7 CFU/ml and 2.44×10^7 CFU/ml. The results indicated that the ZnO-PVDF-HFP coating had a significant antimicrobial effect against *E. coli* and *S. aureus* in ultrasound stimulation, and antibacterial rates were up to 96 %. Compared with the blank control, no antibacterial effect was observed in the PVDF-HFP group, that *E. coli* colonies were 2.02×10^7 CFU/ml and *S. aureus* colonies were 1.95×10^7 CFU/ml. The CFU of the two bacteria in the ZnO NPs group were 0.95×10^7 CFU/ml and 0.9×10^7 CFU/ml. Compared to the blank group, it also has some antimicrobial effect, but the antimicrobial effect was not as pronounced as that of the ZnO-PVDF-HFP + US group. Therefore, the ZnO-PVDF-HFP coated catheter we developed achieves bacterial eradication through the synergistic effect of piezoelectricity and ZnO NPs. The bacterial colonis and bacteriostasis rate in

the other groups were shown in Supplementary Table S1. Then, we measured the absorbance value at 600 nm by a spectrometer to verify the antibacterial ability of the ZnO-PVDF-HFP coated catheters. As shown in Fig. 2B and C, the ZnO-PVDF-HFP coated catheter exhibited excellent antibacterial effect under ultrasonic stimulation.

To further validate the *in vitro* antimicrobial activity, we evaluated the survival status of bacteria in each group using live/dead bacterial staining kits (DMAO/ethD-III). After staining, bacteria with intact cell membranes show green color, while bacteria with damaged cell membranes show red color. The results are shown in Fig. 3A and B. Most of *E. coli* and *S. aureus* in the ZnO-PVDF-HFP + US group were stained with red color, indicating that most bacteria were killed in the group. The red stained bacteria were significantly more than those in other groups. By quantitative analysis of dead bacteria (Fig. 3C and D), dead bacteria of *E. coli* and *S. aureus* in ZnO-PVDF-HFP + US group were 53.7 % and 63.2 %, respectively, which was significantly more than those in other groups too.

Scanning electron microscope of bacterial morphology are shown in Fig. 3E and F. It could be seen that the morphology of *E. coli* and *S. aureus* in the ZnO-PVDF-HFP + US group was severely changed. They lost their morphological integrity, underwent breakage and deformation. The morphological changes of *S. aureus* were a little more obvious, and almost all of the bacteria were broken. The morphology of the bacteria in the PVDF-HFP + US group, ZnO NPs group, ZnO NPs + US group and the ZnO-PVDF-HFP group were all slightly deformed, whereas the morphology of the bacteria in the Blank group, the Blank + US and the PVDF-HFP group was intact. Collectively, it confirmed that ZnO-PVDF-HFP coated catheters showed strong antibacterial ability under ultrasonication against both *E. coli* and *S. aureus*.
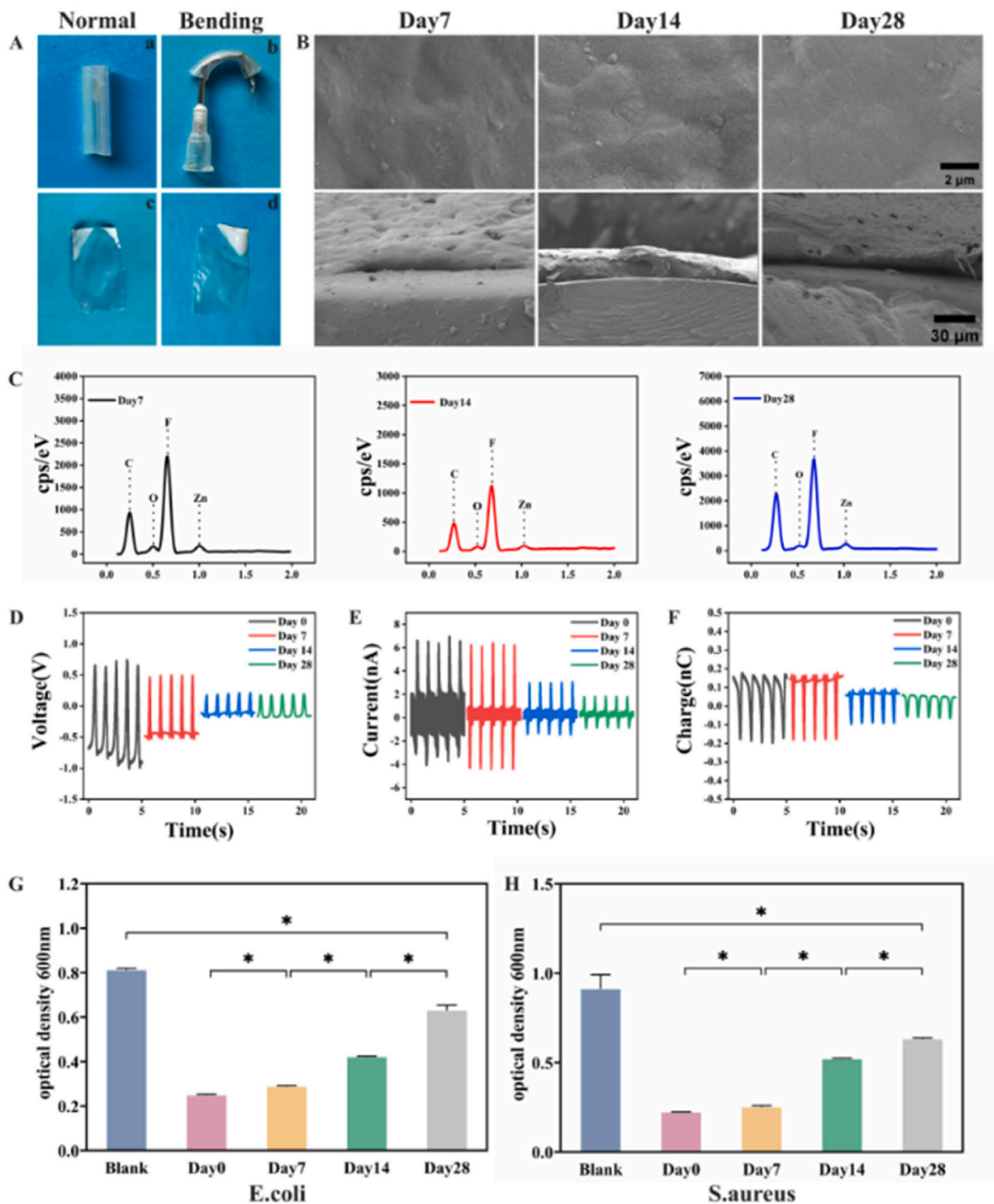
Fig. 4. Stability of ZnO-PVDF-HFP coating. (A) Comparison image of ZnO-PVDF-HFP coated catheter before and after bending, (B) SEM images of ZnO-PVDF-HFP coated catheter after 7, 14, and 28 days of immersion in artificial urine, (C) EDS results, (D) Output voltage, (E) Short-circuit current, (F) Output charge, (G) Optical density value of the immersed catheter after co-culturing with *E. coli* after co-culture with *E. coli*, (H) Optical density value of the bacterial fluid after co-culture of the immersed catheter with *Staphylococcus aureus*. All statistics are expressed as mean ± standard deviation (* indicate statistical differences between coated catheters soaked for different days and untreated catheters; *$P < 0.0001$).

3.3. Stability of ZnO-PVDF-HFP coating

Coating stability is a critical factor that directly affects the performance and safety of catheters. The stability of ZnO-PVDF-HFP on silicone catheter depends on its adhesion ability [36]. Therefore, ensuring good adhesion is the key to maintain the stability of the coating. Coated catheter was cut into small segments for extreme bending under natural conditions, as was shown in Fig. 4A. In the case of folding the catheter in half, the ZnO-PVDF-HFP coating only appeared to be wrinkled but would not peel off. Further, the catheter was cut open to detect the

integrity of ZnO-PVDF-HFP film on catheter, and it was demonstrated that the membrane was not broken. The results indicated that the ZnO-PVDF-HFP coating on the catheter adhered well and could cope with the physiological curvature of the biological urethra. In addition, urine has a complex chemical composition and contains inorganic salts that can affect the function of antimicrobial catheters [37]. Therefore, we immersed the ZnO-PVDF-HFP coated catheters in artificial urine for 0,7, 14, and 28 days for stablity detection. As shown in Fig. 4B and C, no significant difference was observed from SEM on the catheter surface before and after urine soaking. Through the cross-sectional SEM image,
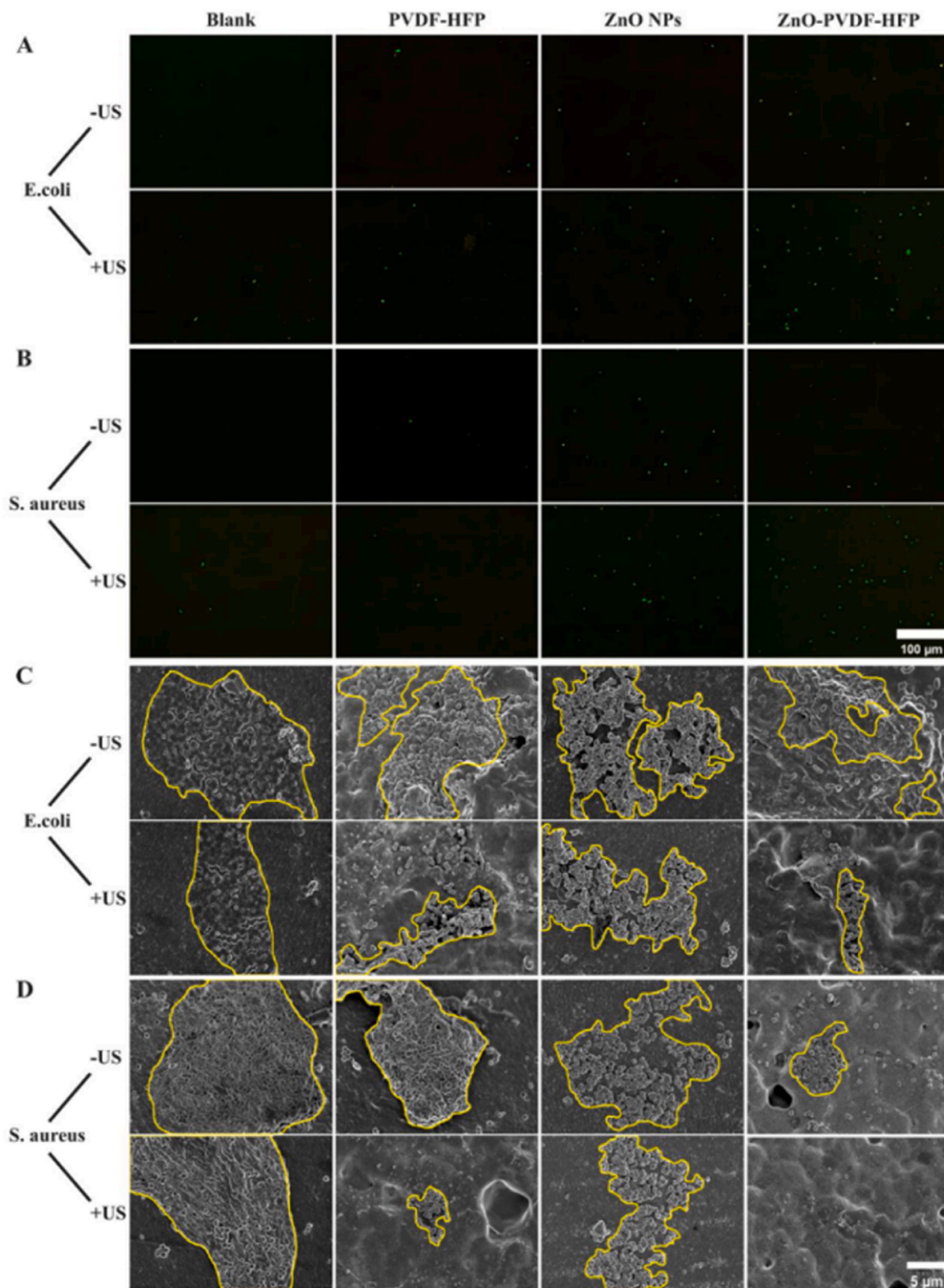
Fig. 5. ROS production and biofilm resistance of different groups of catheters in E. coli and S. aureus. (A and B) ROS staining images of different groups of catheters in *E. coli* and *S. aureus*, (C and D) biofilm SEM images.

a thin film could be still detected on the surface of catheter. The elemental analysis and energy spectroscopy also confirmed the above results. To further verify the stability of the coating, we measured the output voltage, current and charge of the immersed catheter as shown in Fig. 4D-F. It showed that the output voltages of the catheter after 0, 7, 14 and 28 days of immersion were 0.86V, 0.46V, 0.19V and 0.18V; the short-circuit currents were 5.35 nA, 5.32 nA, 2.24 nA, and 1.33 nA; the

output charges were 0.18nc, 0.17 nC, 0.09 nC, and 0.06 nC. We found that if the catheter was immersed in urine within 7 days, its piezoelectric output capacity could be stably maintained. Thereafter, piezoelectricity capacity would be weaken gradually with time, but a significant piezoelectric effect could be produced too even after 28 days.

To detect the antibacterial effect of catheter after urine soaking, the immersed catheters were co-cultured with E.coli and S.aureus. After
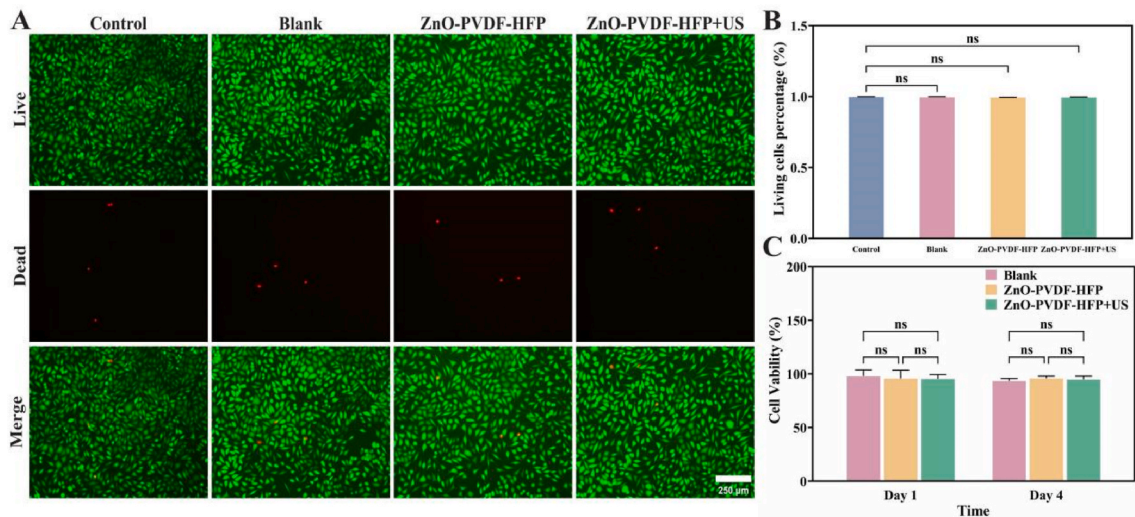
Fig. 6. In vitro biocompatibility and cytotoxicity of ZnO-PVDF-HFP coated catheters. (A) Live/dead stained images, (B) Percentage of live cells on the third day, (C) Cell viability of L929 cells cultured in extracts from ZnO-PVDF-HFP coated catheter. All data are expressed as mean ± standard deviation.

ultrasonic stimulation, the absorbance of bacterial fluid was measured. The results were shown in Fig. 4G and H. A significant antibacterial effect could still be produced after 28 days' urine immersion, though the effect has decreased somewhat.

In most cases, it requires pretreatment to improve coating stability [38]. In contrast, the coating is by PVDF-HFP, which itself adheres well to the surface of the catheter that no other pretreatment is required, resulting in a good stability. The PVDF-HFP coating on catheters was prepared simply by one-step solution film-forming method, which would be convenient and promising for mass production in the future. It should be noted that from 7 days to 28 days of immersion, the piezoelectric properties and antibacterial ability were slightly weakened. We speculate that this may be due to the gradual release of Zn^{2+} from the ZnO-PVDF-HFP coatings with time [39]. Despite, it still has significantly antimicrobial ability after 28days and no detachment of the ZnO-PVDF-HFP membrane from catheters was found. The above results also demonstrate that our ZnO-PVDF-HFP coated catheter has a good stability.

3.4. Antimicrobial mechanism of ZnO-PVDF-HFP coated catheters and their biofilm resistance

ROS are highly active oxygen molecules, including superoxide ions (O^{2-}), hydrogen peroxide (H_2O_2) and hydroxyl radicals $(-OH)$ [40]. Piezoelectric materials can convert mechanical signals into electrical signals upon ultrasonic stimulation. Further, the electrical field can trigger microelectrolysis of water to generate ROS [41]. ROS can be oxidized with microbial biomolecules (such as DNA, proteins and lipids), causing damage to the structure and function of microbial cells, thereby killing microorganisms [42]. Thus, we used 2,7-dichlorofluorescein diacetate (DCFH-DA, a ROS indicator) to determine the ROS production in bacteria. As shown in Fig. 5A, B, a high amount of ROS in both *E. coli* and *S. aureus* was observed in the ZnO-PVDF-HFP + US group, whereas only a small amount of ROS was detected in the ZnO NPs group, ZnO-PVDF-HFP group, PVDF-HFP + US group and the ZnO NPs + US group. No ROS production was found in the Blank group or the simple PVDF-HFP group. This may be why ZnO-PVDF-HFP-coated catheters have a good antibacterial ability under ultrasonic treatment.

Biofilms formed on catheters underlie the pathogenesis of CAUTIs [43]. Bacterial biofilms are complex surface-attached cellular structures embedded in extracellular polymer matrix (EPM). The biofilm EPM mainly consists of polysaccharides, proteins and nucleic acids from the bacteria and the surrounding environment [44]. It contributes to the

strong attachment of bacteria to the surface of the catheter and bacterial resistance to antibiotic treatment. It has been shown that bacterial biofilm generally formed within 7 days after catheter insertion. Therefore, we co-cultured catheters of different treatments with *E. coli* and *S. aureus* for 7 days [45], and biofilm formation was detected through scanning electron microscopy,. As shown in Fig. 5C and D, on the ZnO-PVDF-HFP-coated catheters receiving daily ultrasound treatment, only a small amount of dispersed and damaged *E. coli* and *S. aureus* could be observed. However, in all other groups, different degrees of bacterial aggregation and biofilm formation were detected. Especially, in the blank catheter group, densely formed biofilms were detected. Thus, the piezoelectrically-activated antibacterial catheter in the present study can inhibit biofilm formation in assistance of ultrasonic stimulation.

3.5. Biocompatibility

The biocompatibility of ZnO-PVDF-HFP coatings is an important parameter for evaluating their potential in clinic [46]. The biocompatibility of the coated catheter was tested by cell viability assay using fibroblasts L929. Both Blank catheters and ZnO-PVDF-HFP coated catheters were immersed in cell culture medium. Additionally, the ZnO-PVDF-HFP + US group underwent ultrasound stimulation to simulate actual usage conditions and assess whether ZnO-PVDF-HFP urinary catheters would adversely affect cells. After 24 h, the extracts were extracted and fibroblasts were cultured with the extracts for 1 and 4 days. The cytotoxicity was detected using a live/dead staining (Fig. 6A and B) and CCK-8 kit (Fig. 6C), The results show that the morphology of mammalian cells cultured in the eluate from the ZnO-PVDF-HFP + US group catheters were not altered, and CCK-8 assays showed that ZnO-PVDF-HFP + US group catheters did not affect the viability of fibroblast cells. This indicates that ZnO-PVDF-HFP coated catheters possess excellent biocompatibility.

3.6. Antimicrobial activity of ZnO-PVDF-HFP coated catheters in rabbits

The antimicrobial effect of ZnO-PVDF-HFP coated urinary catheters were evaluated in a rabbit model. Animal experiments were divided into 4 groups, including Control group, Blank group, ZnO-PVDF-HFP group, ZnO-PVDF-HFP + US group. On the 7-day after catheterization, urine samples were collected and diluted 10,000 times. Then, urine bacterial culture were performed and the results are shown in Fig. 7A and B. The average uring bacterial concentration of the control group was 1.4×10^4 CFU/ml. For rabbits inserted with ZnO-PVDF-HFP coated catheters,
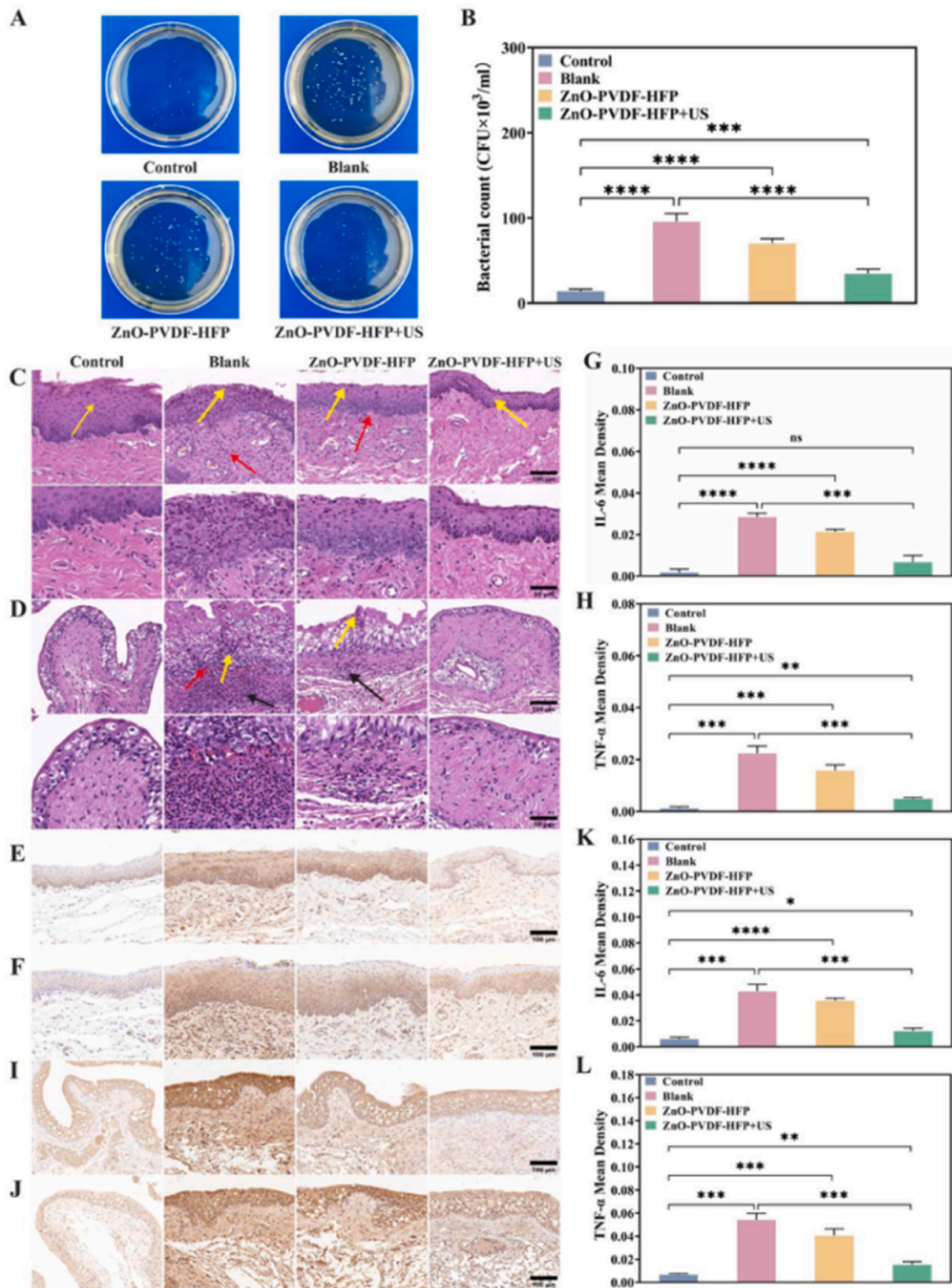
Fig. 7. *In vivo* **antimicrobial effect of different groups of catheters.** (A and B) Urine samples collected from animals for colony counting; (C) H&E staining of rabbit urethra; (D) H&E staining of rabbit bladder; (E and F) Immunohistochemical staining of IL-6 and TNF-α in rabbit urethra; (G and H) Immunohistochemical mean optical density values for IL-6 and TNF-α in rabbit urethra; (I and J) Immunohistochemical staining of IL-6 and TNF-α in rabbit bladder; (K and L) Immunohistochemical mean optical density values for IL-6 and TNF-α in rabbit bladder. All data are expressed as mean ± standard deviation (* indicate statistical differences between different groups of catheters; *$P < 0.05$,**$P < 0.01$,***$P < 0.001$,****$P < 0.0001$).

with the daily ultrasound stimulation, the urine bacterial concentration was 3.5×10^4 CFU/ml which was close to that of the control group, while it was 7×10^4 CFU/ml without ultrasound stimulation. For rabbits inserted with control catheters, the urine bacterial concentration was upto 9.6×10^4 CFU/ml For other groups, rabbits inserted with ZnO-PVDF-HFP coated catheters. Blood tests obtained consistent reslts (Table S2). The number of leukocytes and neutrophils in animals with a blank catheters were higher than normal, indicating that there was a urinary tract infection [47]. In comparison, the leukocytes and neutrophils in rabbits with a ZnO-PVDF-HFP coated catheter were also higher if ultrasonic stimulation was not performed, indicating that ZnO-PVDF-HFP-coated catheter alone could not prevent the development of CAUTIs. Activation of antibacterial ability was necessary, which could be controlled in on-demand manner, on and off, as well as enhanced and weakened.

To evaluate the pathohistological responses after catheter insertion, urethral and bladder tissues were collected for H&E and immunohistochemical staining. The results were shown in Fig. 7C. Complete and orderly arranged epithelial cells could be observed in the Control group of rabbit urethral tissue (yellow arrows), and a large number of collagen fibers were visible in the lamina propria. No obvious inflammatory cell infiltration was observed. In the Blank catheter group, the epithelial cells were arranged in a disordered way (yellow arrow), and the collagen fibers in the lamina propria were loosely arranged(red arrow). Meanwhile, a large amount of granulocyte infiltration was seen in both the epithelial and lamina propria, indicating that the emergence of urinary tract infection. In the ZnO-PVDF-HFP catheter group, the epithelial cells were arranged in a more intact way, and collagen fibers in the lamina propria were loosely arranged. A small amount of granulocyte infiltration could be seen in the tissues, and the degree of inflammation was significantly relieved compared with the Blank catheter group. The tissue structure of ZnO-PVDF-HFP + US group was nearly normal. that the epithelial cells were completely arranged, the collagen fibers of the lamina propria were tightly arranged, and no obvious inflammatory cell infiltration was seen in the tissue. Analysis of bladder tissue was shown in Fig. 7D. For control group, complete arrangement of migrating epithelium was ovserved in bladder tissues, no obvious degeneration and shedding. Abundant distribution of collagen fibers could be observed in the lamina propria, no inflammatory cell infiltration. In the blank catheter group, the tissue structure was severely changed. collagen fibers were significantly reduced in the lamina propria and a large number of granulocyte infiltration appeared as shown by the black arrowheads. It could also be seen some inflammatory cells infiltrated into the epithelium (yellow arrowheads), and a large number of microvessels were dilated and congested (red arrowheads). In the ZnO-PVDF-HFP catheter group, the tissue structure was also somewhat changed, that collagen fibers were sparsely arranged in the lamina propria and a small amount of granulocyte infiltration was observed. In the ZnO-PVDF-HFP + US group, the tissue structure was basically normal, the epithelial cells were well arranged, and the lamina propria was not infiltrated with obvious inflammatory cells (black arrows). The above results consistently confirmed that ZnO-PVDF-HFP coated catheters can effectively inhibit bacterial growth and prevent the occurrence of catheter-associated urinary tract infections in animals with the assistence of ultrasonic stimulation.

Further, we detected the expression of IL-6 and TNF-α in the rabbit model by immunohistochemical (IHC) staining [48,49]. As shown in Fig. 7E–H, low levels of IL-6 and TNF-α staining were observed in the normal urethra and bladder tissues. However, in the blank catheter group, high levels of IL-6 and TNF-α staining were observed. In comparison, IL-6 and TNF-α in the ZnO-PVDF-HFP + US group was significantly reduced. Then, quantative analysis of IL-6 and TNF-α was performed by measuring the average optical density values of the immunostaining (Fig. 7I-L). There was no significant difference between the ZnO-PVDF-HFP + US group and the control group, but significantly higher expression of IL-6 and TNF-α were found in both the blank

catheter group and the ZnO-PVDF-HFP group than that of control. The above results provided additional evidence that the piezoelectrically-activated antibacterial catheter (ZnO-PVDF-HFP coated catheter) can prevent the occurrence of urinary tract infection under ultrasonic stimulation.

4. Conclusion

In the study, we developed a piezoelectrically-activated antimicrobial catheters by coating ZnO-PVDF-HFP with one-step film-forming method. *In vitro*, the ZnO-PVDF-HFP antimicrobial coating significantly inhibited bacteria and biofilm formation. Meanwhile, the ZnO-PVDF-HFP antimicrobial coating proved to be of good stability and biocompatibility *in vitro* and in vivo. Further, experiments in rabbits revealed that the ZnO-PVDF-HFP antibacterial catheter significantly reduced the pathogen growth in the urinary tract and thus prevented CAUTIs with the assistance of ultrosonic stimulation. More importantly, the on and off of antimicrobial activity as well as the strenth of antibacterial property could be controlled in on-demand manner, adaptive to infection situation and promising in clinical application.

Ethics approval and consent to participate

The authors declare that all animal experiments are approved by the Institutional Animal Care and Use Committee (IACUC-JSRZ-23-0401) as well as the ARRIVE Guidelines. All authors comply with all relevant ethical regulations.

CRediT authorship contribution statement

Xiaofeng Duan: Writing – original draft, Resources, Methodology, Investigation, Funding acquisition, Formal analysis, Data curation, Conceptualization. **Yongde Xu:** Writing – original draft, Methodology, Formal analysis. **Zhifa Zhang:** Investigation, Data curation. **Xinbo Ma:** Investigation, Data curation. **Cui Wang:** Supervision, Formal analysis. **Wenjing Ma:** Supervision, Conceptualization. **Fan Jia:** Methodology, Formal analysis. **Xiaoying Pan:** Validation. **Yang Liu:** Validation. **Yantao Zhao:** Supervision, Resources. **Qihong Li:** Supervision, Resources. **Zhiqiang Liu:** Writing – review & editing, Supervision, Resources, Funding acquisition. **Yong Yang:** Writing – review & editing, Supervision, Resources, Funding acquisition.

Declaration of competing interest

The authors declare that they have no known competing financial interests or personal relationships that could have appeared to influence the work reported in this paper.

Data availability

Data will be made available on request.

Appendix A. Supplementary data

Supplementary data to this article can be found online at https://doi.org/10.1016/j.mtbio.2024.101089.

References

[1] C.M.C. Faustino, S.M.C. Lemos, N. Monge, et al., A scope at antifouling strategies to prevent catheter-associated infections, Adv. Colloid Interface Sci. 284 (2020) 102230, https://doi.org/10.1016/j.cis.2020.102230.

[2] C.E. Chenoweth, S. Saint, Urinary tract infections, Infect Dis Clin North Am 25 (1) (2011) 103–115, https://doi.org/10.1016/j.idc.2010.11.005.

[3] L.E. Nicolle, Urinary catheter-associated infections, Infect Dis Clin North Am 26 (1) (2012) 13–27, https://doi.org/10.1016/j.idc.2011.09.009.

[4] S.S. Magill, J.R. Edwards, W. Bamberg, et al., Multistate point-prevalence survey of health care-associated infections, N. Engl. J. Med. 370 (13) (2014) 1198–1208, https://doi.org/10.1056/NEJMoa1306801.

[5] J. Kranz, S. Schmidt, F. Wagenlehner, et al., Catheter-associated urinary tract infections in adult patients, Dtsch Arztebl Int 117 (6) (2020) 83–88, https://doi.org/10.3238/arztebl.2020.0083.

[6] A.S.A. Lila, A.A.H. Rajab, M.H. Abdallah, et al., Biofilm lifestyle in recurrent urinary tract infections, Life 13 (1) (2023), https://doi.org/10.3390/life13010148.

[7] S. Rajaramon, K. Shanmugam, R. Dandela, et al., Emerging evidence-based innovative approaches to control catheter-associated urinary tract infection: a review, Front. Cell. Infect. Microbiol. 13 (2023) 1134433, https://doi.org/10.3389/fcimb.2023.1134433.

[8] S. Navarro, E. Sherman, J.A. Colmer-Hamood, et al., Urinary catheters coated with a novel biofilm preventative agent inhibit biofilm development by diverse bacterial uropathogens, Antibiotics (Basel) 11 (11) (2022), https://doi.org/10.3390/antibiotics11111514.

[9] B. McVerry, A. Polasko, E. Rao, et al., A readily scalable, clinically demonstrated, antibiofouling zwitterionic surface treatment for implantable medical devices, Adv. Mater. 34 (20) (2022) e2200254, https://doi.org/10.1002/adma.202200254.

[10] S. Zhang, L. Wang, X. Liang, et al., Enhanced antibacterial and antiadhesive activities of silver-PTFE nanocomposite coating for urinary catheters, ACS Biomater. Sci. Eng. 5 (6) (2019) 2804–2814, https://doi.org/10.1021/acsbiomaterials.9b00071.

[11] J.R. Johnson, M.A. Kuskowski, T.J. Wilt, Systematic review: antimicrobial urinary catheters to prevent catheter-associated urinary tract infection in hospitalized patients, Ann. Intern. Med. 144 (2) (2006) 116–126, https://doi.org/10.7326/0003-4819-144-2-200601170-00009.

[12] B.W. Trautner, R.O. Darouiche, Role of biofilm in catheter-associated urinary tract infection, Am. J. Infect. Control 32 (3) (2004) 177–183, https://doi.org/10.1016/j.ajic.2003.08.005.

[13] K. Li, H. Tang, J. Peng, et al., Smart lubricant coating with urease-responsive antibacterial functions for ureteral stents to inhibit infectious encrustation, Adv. Funct. Mater. 34 (2) (2024) 2307760, https://doi.org/10.1002/adfm.202307760.

[14] J.F. Dubern, A.L. Hook, A.M. Carabelli, et al., Discovery of a polymer resistant to bacterial biofilm, swarming, and encrustation, Sci. Adv. 9 (4) (2023) eadd7474, https://doi.org/10.1126/sciadv.add7474.

[15] M.J. Andersen, C. Fong, A.A. La Bella, et al., Inhibiting host-protein deposition on urinary catheters reduces associated urinary tract infections, Elife 11 (2022), https://doi.org/10.7554/eLife.75798.

[16] P. Singha, J. Locklin, H. Handa, A review of the recent advances in antimicrobial coatings for urinary catheters, Acta Biomater. 50 (2017) 20–40, https://doi.org/10.1016/j.actbio.2016.11.070.

[17] T.B. Lam, M.I. Omar, E. Fisher, et al., Types of indwelling urethral catheters for short-term catheterisation in hospitalised adults, Cochrane Database Syst. Rev. (9) (2014) Cd004013, https://doi.org/10.1002/14651858.CD004013.pub4.

[18] K. Li, J. Peng, Y. Liu, et al., Surface engineering of central venous catheters via combination of antibacterial endothelium-mimicking function and fibrinolytic activity for combating blood stream infection and thrombosis, Adv. Healthcare Mater. 12 (23) (2023) e2300120, https://doi.org/10.1002/adhm.202300120.

[19] E.M.J. Lin, C.L. Lay, G.S. Subramanian, et al., Control release coating for urinary catheters with enhanced released profile for sustained antimicrobial protection, ACS Appl. Mater. Interfaces 13 (49) (2021) 59263–59274, https://doi.org/10.1021/acsami.1c17697.

[20] J. Miao, X. Wu, Y. Fang, et al., Multifunctional hydrogel coatings with high antimicrobial loading efficiency and pH-responsive properties for urinary catheter applications, J. Mater. Chem. B 11 (15) (2023) 3373–3386, https://doi.org/10.1039/d3tb00148b.

[21] L. Duque-Sanchez, Y. Qu, N.H. Voelcker, et al., Tackling catheter-associated urinary tract infections with next-generation antimicrobial technologies, J. Biomed. Mater. Res. 112 (3) (2024) 312–335, https://doi.org/10.1002/jbm.a.37630.

[22] L. Sun, X. Chen, K. Ma, et al., Novel titanium implant: a 3D multifunction architecture with charge-trapping and piezoelectric self-stimulation, Adv. Healthcare Mater. 12 (11) (2023) e2202620, https://doi.org/10.1002/adhm.202202620.

[23] J. Moreira, M.M. Fernandes, E.O. Carvalho, et al., Exploring electroactive microenvironments in polymer-based nanocomposites to sensitize bacterial cells to low-dose embedded silver nanoparticles, Acta Biomater. 139 (2022) 237–248, https://doi.org/10.1016/j.actbio.2021.07.067.

[24] A. Biswas, D.V. Bhalani, G. Bhojani, et al., Poly(vinylidene fluoride)/partially alkylated poly(vinyl imidazole) interpolymer ultrafiltration membranes with intrinsic anti-biofouling and antifouling property for the removal of bacteria, J. Hazard Mater. 438 (2022) 129538, https://doi.org/10.1016/j.jhazmat.2022.129538.

[25] D. Liu, L. Li, B.L. Shi, et al., Ultrasound-triggered piezocatalytic composite hydrogels for promoting bacterial-infected wound healing, Bioact. Mater. 24 (2023) 96–111, https://doi.org/10.1016/j.bioactmat.2022.11.023.

[26] Y. Li, L. Sun, T.J. Webster, The investigation of ZnO/Poly(vinylidene fluoride) nanocomposites with improved mechanical, piezoelectric, and antimicrobial properties for orthopedic applications, J. Biomed. Nanotechnol. 14 (3) (2018) 536–545, https://doi.org/10.1166/jbn.2018.2519.

[27] P. Huang, S. Xu, W. Liu, et al., ZnO@Carbon dot nanoparticles stimulating the antibacterial activity of polyvinylidene fluoride-hexafluoropropylene with a higher electroactive phase for multifunctional devices, ACS Appl. Mater. Interfaces 15 (5) (2023) 6735–6746, https://doi.org/10.1021/acsami.2c18859.

[28] Z. He, F. Rault, M. Lewandowski, et al., Electrospun PVDF nanofibers for piezoelectric applications: a review of the influence of electrospinning parameters on the β phase and crystallinity enhancement, Polymers 13 (2) (2021), https://doi.org/10.3390/polym13020174.

[29] M.J. Islam, H. Lee, K. Lee, et al., Piezoelectric nanogenerators fabricated using spin coating of poly(vinylidene fluoride) and ZnO composite, Nanomaterials 13 (7) (2023), https://doi.org/10.3390/nano13071289.

[30] D. Mandal, K. Henkel, D. Schmeisser, Improved performance of a polymer nanogenerator based on silver nanoparticles doped electrospun P(VDF-HFP) nanofibers, Phys. Chem. Chem. Phys. 16 (22) (2014) 10403–10407, https://doi.org/10.1039/c3cp55238a.

[31] M. Zhang, Z. Tan, Q. Zhang, et al., Flexible self-powered friction piezoelectric sensor based on structured PVDF-based composite nanofiber membranes, ACS Appl. Mater. Interfaces 15 (25) (2023) 30849–30858, https://doi.org/10.1021/acsami.3c05540.

[32] Z.X. Wang, H. Zhang, F. Wang, et al., Superior transverse piezoelectricity in a halide perovskite molecular ferroelectric thin film, J. Am. Chem. Soc. 142 (29) (2020) 12857–12864, https://doi.org/10.1021/jacs.0c06064.

[33] G.S. Kumar, D. Vishnupriya, K.S. Chary, et al., High dielectric permittivity and improved mechanical and thermal properties of poly(vinylidene fluoride) composites with low carbon nanotube content: effect of composite processing on phase behavior and dielectric properties, Nanotechnology 27 (38) (2016) 385702, https://doi.org/10.1088/0957-4484/27/38/385702.

[34] Y. Su, W. Li, X. Cheng, et al., High-performance piezoelectric composites via β phase programming, Nat. Commun. 13 (1) (2022) 4867, https://doi.org/10.1038/s41467-022-32518-3.

[35] T.M. Nye, Z. Zou, C.L.P. Obernuefemann, et al., Microbial co-occurrences on catheters from long-term catheterized patients, Nat. Commun. 15 (1) (2024) 61, https://doi.org/10.1038/s41467-023-44095-0.

[36] K.Z. Walle, Y.S. Wu, S.H. Wu, et al., Lithium nafion-modified Li(6.05)Ga(0.25)La (3)Zr(2)O(11.8)F(0.2) trilayer hybrid solid electrolyte for high-voltage cathodes in all-solid-state lithium-metal batteries, ACS Appl. Mater. Interfaces 14 (13) (2022) 15259–15274, https://doi.org/10.1021/acsami.2c00753.

[37] K. Ivanova, M.M. Fernandes, A. Francesko, et al., Quorum-quenching and matrix-degrading enzymes in multilayer coatings synergistically prevent bacterial biofilm formation on urinary catheters, ACS Appl. Mater. Interfaces 7 (49) (2015) 27066–27077, https://doi.org/10.1021/acsami.5b09489.

[38] P. Petkova, A. Francesko, M.M. Fernandes, et al., Sonochemical coating of textiles with hybrid ZnO/chitosan antimicrobial nanoparticles, ACS Appl. Mater. Interfaces 6 (2) (2014) 1164–1172, https://doi.org/10.1021/am404852d.

[39] C.A. David, J. Galceran, F. Quattrini, et al., Dissolution and phosphate-induced transformation of ZnO nanoparticles in synthetic saliva probed by AGNES without previous solid-liquid separation. Comparison with UF-ICP-MS, Environ. Sci. Technol. 53 (7) (2019) 3823–3831, https://doi.org/10.1021/acs.est.8b06531.

[40] Y. Zhang, Q. An, S. Zhang, et al., A healing promoting wound dressing with tailor-made antibacterial potency employing piezocatalytic processes in multi-functional nanocomposites, Nanoscale 14 (7) (2022) 2649–2659, https://doi.org/10.1039/d1nr07386a.

[41] S. Chen, P. Zhu, L. Mao, et al., Piezocatalytic medicine: an emerging frontier using piezoelectric materials for biomedical applications, Adv. Mater. 35 (25) (2023) e2208256, https://doi.org/10.1002/adma.202208256.

[42] Z. Wen, X. Shi, X. Li, et al., Mesoporous TiO(2) coatings regulate ZnO nanoparticle loading and Zn(2+) release on titanium dental implants for sustained osteogenic and antibacterial activity, ACS Appl. Mater. Interfaces 15 (12) (2023) 15235–15249, https://doi.org/10.1021/acsami.3c00812.

[43] Y. Kurmoo, A.L. Hook, D. Harvey, et al., Real time monitoring of biofilm formation on coated medical devices for the reduction and interception of bacterial infections, Biomater. Sci. 8 (5) (2020) 1464–1477, https://doi.org/10.1039/c9bm00875f.

[44] K.J. Wynne, O. Zolotarskaya, R. Jarrell, et al., Facile modification of medical-grade silicone for antimicrobial effectiveness and biocompatibility: a potential therapeutic strategy against bacterial biofilms, ACS Appl. Mater. Interfaces 15 (40) (2023) 46626–46638, https://doi.org/10.1021/acsami.3c08734.

[45] S. Amin Yavari, S.M. Castenmiller, J.A.G. van Strijp, et al., Combating implant infections: shifting focus from bacteria to host, Adv. Mater. 32 (43) (2020) e2002962, https://doi.org/10.1002/adma.202002962.

[46] A.P. Nagvenkar, I. Perelshtein, Y. Piunno, et al., Sonochemical one-step synthesis of polymer-capped metal oxide nanocolloids: antibacterial activity and cytotoxicity, ACS Omega 4 (9) (2019) 13631–13639, https://doi.org/10.1021/acsomega.9b00181.

[47] K. Eislmayr, A. Bestehorn, L. Morelli, et al., Nonredundancy of IL-1α and IL-1β is defined by distinct regulation of tissues orchestrating resistance versus tolerance to

infection, Sci. Adv. 8 (9) (2022) eabj7293, https://doi.org/10.1126/sciadv. abj7293.

[48] J. Qu, X. Zhao, Y. Liang, et al., Antibacterial adhesive injectable hydrogels with rapid self-healing, extensibility and compressibility as wound dressing for joints

skin wound healing, Biomaterials 183 (2018) 185–199, https://doi.org/10.1016/j. biomaterials.2018.08.044.

[49] Y. Liang, J. He, B. Guo, Functional hydrogels as wound dressing to enhance wound healing, ACS Nano 15 (8) (2021) 12687–12722, https://doi.org/10.1021/ acsnano.1c04206.